Bulk microstructure in a strained cohesive powder

R. Andersson,[1,*] W.G. Bouwman,[1] S. Luding,[2] and I.M. de Schepper[1]

[1] *Radiation, Radionuclides & Reactors, Delft University of Technology, Mekelweg 15, 2629JB Delft, the Netherlands*
[2] *Multi Scale Mechanics, Department of Mechanical Engineering, University of Twente, P.O. Box 217, 7500AE Enschede, the Netherlands*

(Dated: December 21, 2007)

Spin-Echo Small Angle Neutron Scattering is able to characterise powders in terms of their density-density correlation function. Here we present a micro-structural study on a fine cohesive powder undergoing uniaxial compression. As a function of compression we measure the autocorrelation function of the density distribution. From these measurements we quantify the typical sizes of the heterogeneities as well as the fractal nature of the powder packing. The fractal dimension is increasing with increasing stress, creating a more space-filling structure. The typical size of the heterogeneities is found to decrease nonlinearly with increasing compressive strain. In this way we link the macroscopic mechanical response with the evolution of microstructure inside the bulk of the cohesive powder. We find that the total macroscopic compressive strain is in agreement with a corresponding decrease in microstructural length scales.

PACS numbers: 61.43.Gt, 61.43.Hv, 61.12.Ex, 81.05.Rm
Keywords: Powder, Cohesion, Microstructure, Small-Angle Neutron Scattering, SESANS

I. INTRODUCTION

Rather than being driven by the hard-core exclusion between grains, the structure of cohesive powders is mainly determined by van der Waals attraction amongst small primary particles (<100μm). As a result of these adhesive forces, and the irrelevancy of body forces, very loosely packed and fluffy structures are seen to form in these materials. The structures lead to process related issues relevant to industry in a sense that mass flows become unstable [1]. An increased demand for particulate materials in the nanoscale makes the understanding of these type of granular materials important.

To precisely understand the macroscopic behaviour of powders, the computer-modelling and theory-buildup needs the support of experiments on realistic samples. More specifically, there is a need for experiments that can quantify powders in terms of their microstructure. Experiments are needed that can look inside the 'fluffy' structure of cohesive powders so that more quantitative statements can be made.

Extracting information from the bulk of powders and granular materials is difficult. The opacity and the wide range of sizes present in real materials renders most optical and conventional wave diffraction techniques more or less useless. The opacity can be overcome by using some penetrating radiation such as x-rays in x-ray tomography [2–4] or radio-waves in Magnetic Resonance Imaging [5, 6].

Spin Echo Small Angle Neutron Scattering (SESANS) is using the penetrating ability of neutrons, where the measured signal is a real space correlation function of the sample inhomogeneities [7]. SESANS is used to probe the structure across three orders of magnitude ranging from 30nm up to 20μm, making it applicable to fine cohesive powders [8], colloidal systems [9], dairy products [10], just to name a few.

The autocorrelation function of the density distribution $\gamma(r)$ is a convenient way to statistically characterise the microstructure of heterogeneous materials. This function is measured in a small-angle scattering experiment as its Fourier transform (the so called structure/form factor). SESANS is measuring $\gamma(r)$ via its projection along the neutron beam path, making SESANS a real-space technique. The typical size, packing fraction, any anisotropy, scale invariance and ordering of the sample heterogeneities are examples of extractable characteristics.

Here we have performed a stress-strain measurement on a fine cohesive silica powder together with consecutive SESANS measurements. In the analysis, the cohesive powder is considered as being a self-affine random two-phase material. We use a model function for the density-density correlation function containing a typical length scale and a Hurst number related to the fractal dimension of the structure [11, 12].

From the initial decay of the measured curve we extract the unknown primary grain density and consequently the grain packing fraction. Furthermore, we find that the typical size of the inhomogeneities decays in a non linear way with increasing compressive strain. The Hurst number is seen to decrease towards zero with increasing stress and strain, showing that a more space filling structure is formed as the powder packing is compacted. All together this microstructural investigation provides insight in the fractal nature of fine cohesive powders as well as on the non-linear behaviour between 'microscales' and macroscopic mechanics.

*r.a.andersson@tudelft.nl

II. STRUCTURE AND SESANS

A. On the density distribution and its correlation function

The density distribution, $\rho(r)$, in a heterogeneous two phase sample is expected to fluctuate around its mean value. These fluctuations might be characterised by some typical size, anisotropy, being fractal or self affine, regular (crystalline), random and so on. All together, this is what we call the structure of a material. The structure of two phase systems such as a powder material can be analysed by taking the autocorrelation function of its density distribution:

$$C(r) = \langle \Delta\rho(0)\Delta\rho(r)\rangle \tag{1}$$

where the mean, $\bar{\rho}$, has been subtracted ($\Delta\rho(r) = \rho(r) - \bar{\rho}$). The mean square fluctuation is

$$C(0) = \Delta\rho_0\phi_1\phi_2 \tag{2}$$

Where $\phi_1 + \phi_2$=1 is the packing-fractions of the two phases and $\Delta\rho_0 = \rho_1 - \rho_2$ is the density difference between the two phases. The normalised (dimensionless) correlation function is the so called density-density correlation function:

$$\gamma(r) = \frac{C(r)}{C(0)}. \tag{3}$$

The projection of $\gamma(r)$ is given by:

$$G(z) = \frac{2}{\xi}\int_z^\infty \frac{r\gamma(r)}{\sqrt{r^2 - z^2}}dr \tag{4}$$

in Cartesian coordinates:

$$G(z) = \frac{1}{\xi}\int_{-\infty}^{\infty} \gamma(x, 0, z)dx. \tag{5}$$

The projection is made dimensionless with the correlation length of the density distribution [13].

$$\xi = \int_{-\infty}^{\infty} \gamma(r)dr \tag{6}$$

so that $G(0) = 1$.

B. Spin-Echo Small Angle Neutron Scattering (SESANS)

Spin-echo Small Angle Neutron scattering (SESANS) is based on the Larmor-precession of neutrons in parallelogram shaped magnetic field regions [14], [15]. In SESANS, the polarisation of a neutron beam is measured, after transmission through a sample, as a function of the so called spin-echo length (30nm$<z<$20μm). The spin-echo length is a real-space parameter representing the size at which the correlations are measured (in the z-direction of the lab-coordinate system). In SESANS we measure $G(z)$ through the transmission of polarisation, normalised with experimental effects, as a function of z.

$$P(z) = e^{\Sigma_t(G(z)-1)}, \tag{7}$$

where

$$\Sigma_t = t\lambda^2\Delta\rho_0^2\phi_1\phi_2\xi. \tag{8}$$

Here t is the sample thickness, λ the neutron wavelength and $\Delta\rho_0$ is the neutron scattering-length density difference in the sample (i.e., the contrast between the two phases in the sample).

The correlation length ξ is measured along the neutron beam-axis of a SESANS experiment, which is perpendicular to the z direction. ξ is a measure of the width of the distribution $\gamma(r)$, which is in principle a measure of the size of the inhomogeneities in the sample (for a sphere the correlation length is 3/4 of the sphere-diameter). It can be interpreted as the mean-free-path of a neutron in the sample.

At large z (above the typical size of the heterogeneities) one expects no more correlations ($G(\infty) = 0$), this gives a so called saturation level of the polarisation:

$$P(\infty) = e^{-\Sigma_t}. \tag{9}$$

Thus, the polarisation at saturation is proportional the correlation length ξ of the sample-inhomogeneities.

C. Correlation function of a random two-phase system

A cohesive powder is a particular case of a two phase system that is heterogeneous at (most likely) many scales. The attractive forces between grain pairs allow the build up of connected networks and aggregates of low coordination number, resulting in large voids of air pockets and low densities. In the end we have in mind a very porous material carrying a low packing fraction of grains that will be far from a random close packing of hard-spheres.

For a perfectly random heterogeneous material made up of 3D solids bounded by smooth 2D surfaces the density-density correlation function can be described by the so called Debye-Andersson-Bueche (DAB) formalism [16–18]:

$$\gamma_{DAB}(r) = e^{-r/a} \tag{10}$$

where a is a measure of the typical size of the heterogeneities. This function is in fact a special case the more general von Karman correlation function [11, 19]:

$$\gamma_K(r) = \frac{2}{\Gamma(H)} \left(\frac{r}{2a}\right)^H K_H \left(\frac{r}{a}\right), \quad (11)$$

where $0 < H < 1$ is the so called Hurst exponent, related to the dimensionality of the structure. The limits $H = 0$ and $H = 1$ correspond to space filling and smooth Euclidian distributions respectively (see Fig. 1). K_H is the second order modified Bessel function and Γ is the gamma function. For $H = 1/2$ this simplifies to the DAB formula (in 1D such distribution function is neither persistent nor anti-persistent, it is a memoryless Markov chain).

A 1D reconstruction of von Karman density distributions for various H : s can be seen in Fig. 1. A low Hurst exponent correspond to a high space filling capacity and unity correspond to the Euclidian structure (a smooth line in the example in Fig. 1). The reconstruction depicted here is done in reciprocal space followed by inverse fast fourier transformation [11] in order to get the spatial domain representation.

The projection of Eq. 11 is found by insertion in Eq. 4, which leads too

$$G_K(z) = \frac{2}{\Gamma(H+1/2)} \left(\frac{z}{2a}\right)^{H+1/2} K_{H+1/2} \left(\frac{z}{a}\right). \quad (12)$$

The corresponding correlation length for such density distribution will be:

$$\xi_K = \frac{2\sqrt{\pi}a\Gamma(H+1/2)}{\Gamma(H)}, \quad (13)$$

In conventional small angle neutron scattering one measures the Fourier transform of Eq. 11 which yields the normalised structure factor

$$I(q) = \frac{1}{(1+(qa)^2)^{\frac{3}{2}+H}}, \quad (14)$$

III. EXPERIMENTS AND SAMPLE PROPERTIES

A powder sample was kindly provided by Degussa (www.degussa.com). The product is called Sipernat-310, which is a synthetic-precipitated silica used in coatings, cosmetics, cements, rubbers, as filler etc. It is a typical cohesive powder containing fine grains around 5μm. The sample was used without any further treatment in ambient conditions.

We have used the SESANS setup at the Reactor Institute Delft (Delft University of Technology in the Netherlands) to perform the measurements. The instrument

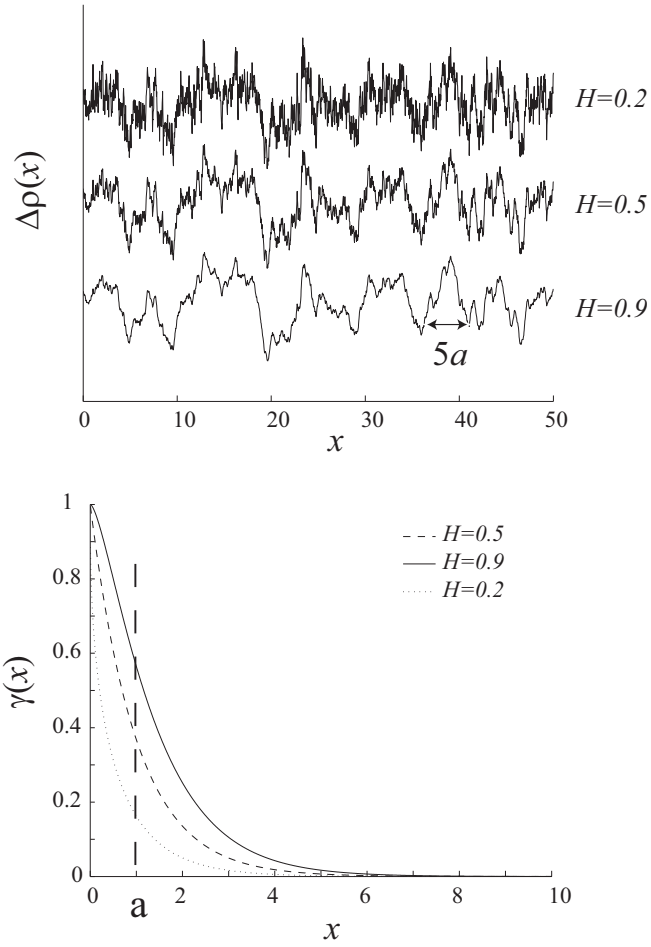

FIG. 1: The top figure shows examples of reconstructed 1D density distributions $\rho(x)$ based on the von Karman correlation function Eq. 11. The corresponding correlation functions are shown in the bottom figure. The characteristic size is here a=1

contains two parallelogram-shaped magnetic field regions with opposite magnetic induction direction (otherwise identical). The sample is positioned between the field regions. Any neutron scattering between the two fields will break the symmetry of the setup and cause the beam to depolarise. The strength of the field defines the so called spin-echo length z, which will be perpendicular to the beam direction and pointing in the direction of gravity. The polarisation of the neutron beam is measured as a function z. The beam is nearly monochromatic with a wavelength of 0.21nm having a cross section at the sample position around 1cm^2.

A simple uniaxial load-cell was used in order to measure the stress versus strain function of the powder (see Fig. 2). Strain we define as being the relative decrease in thickness of the sample $((t_0 - t)/t_0)$ achieved by the applied stress. The stress/strain tester contains a cylindrical cavity with a movable hollow plunger that achieves the compression inside the cavity. The plunger was

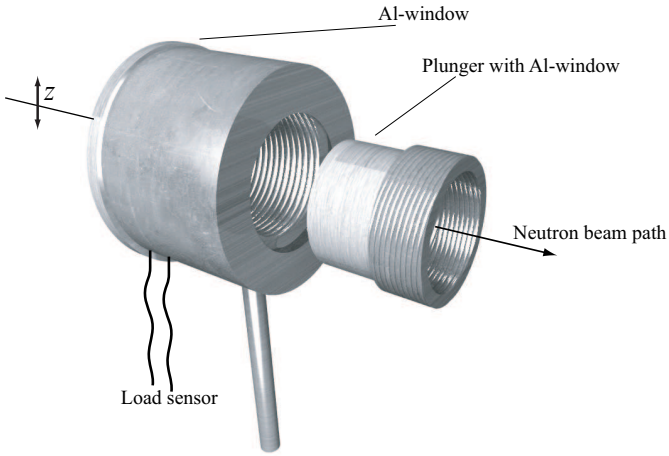

FIG. 2: This figure is illustrating the load cell used in the stress-strain measurements on the cohesive powder. The initial height of the powder packing was 6.5mm and subsequently strained by nine increments of 0.25mm. The stress was measured using Flexiforce load sensors situated at the first Al-window.

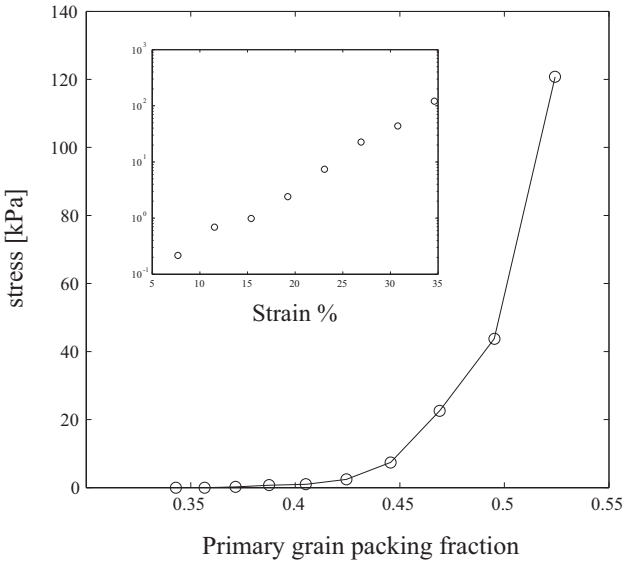

FIG. 3: The stress versus grain packing-fraction relationship. The inset shows a linear relationship between the logarithm of the stress versus strain. Note that the first two points yielded no measurable stress on the Flexiforce load sensors.

moved by a separate screwing action (without rotating the plunger) until a desired incremental strain was reached. We used nine increments of 0.25mm with an initial powder height of 6.5mm. The cylindrical cavity and the plunger are sealed off with aluminium windows (aluminium is virtually transparent to neutrons). The absolute stress was measured with Flexiforce load sensors provided by Tekscan (www.tekscan.com).

The initial powder packing is a very soft, low-density material and easily compacted (weakly aggregated). As seen in the stress-strain curve, which shows a exponential behaviour in the probed interval (Fig. 3).

IV. RESULTS AND DISCUSSION

A. First interpretation

When analysing the measurements it is often useful to interpret what we simply see by eye. In Fig. 4 we see the polarisation plotted as a function of z. In total, ten measurements at ten different strain levels was carried out. We show only four measurements for the sake of clarity, otherwise the trends are consistent for all ten incremental strains.

Increasing the strain moves the saturation polarisation upwards, thus the upper lying curves correspond to higher stress and strain than the lower ones. Increasing the strain makes the powder packing denser (ϕ) and thinner (t), both contributing to less scattering and higher polarisation saturation levels.

The second microstructural parameter contributing to the end level is the correlation length ξ. We argue that the rearrangement of particles into a denser state must decrease the size of the heterogeneities (despite the formation of force chains), giving a lower correlation length with increasing strain. Such decrease would also contribute to higher saturation polarisation levels.

At saturation we are able to read off the largest correlating size of the microstructure on the horizontal-axis. The measurement saturates around 5μm, being the size of grains making up the powder.

The stress versus strain curve can be seen in Fig. 3.T he curve shows that when plotting the logarithm of the stress versus strain we have a linear relationship. The powder is at its native state a very soft powder with low density stabilised by adhesive forces in the form of capillary and van der Waals forces. The hard core exclusion between the silica grains finally makes the powder more resistant to compaction in a exponential fashion.

B. Linear initial slopes

The powder is composed of grains having an unknown density and the grain density is expected to be lower as compared with the solid density of pure silica (2.2-2.5g/cm^3). From a primary grain density we are able to obtain the grain packing fraction ϕ_{grain} rather than the skeleton packing fraction ϕ_{sk} calculated from solid silica density. This density can be determined from the measurement by analysing the initial slope of the polarisation vs z curves.

$$\phi_{sk} = \frac{\rho_{sample}}{\rho_{SiO_2}} \tag{15}$$

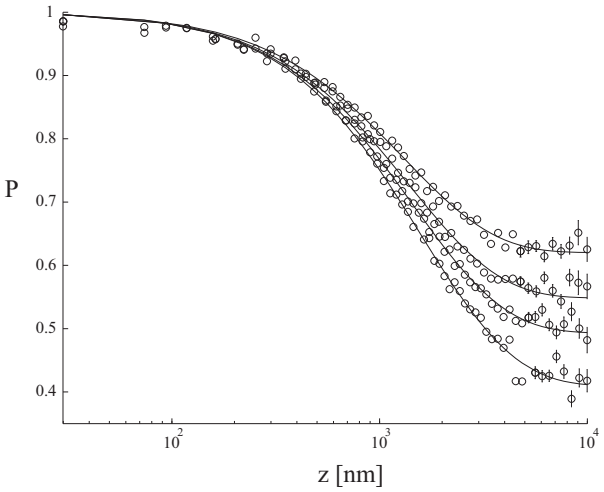

FIG. 4: Polarisation plotted as a function of z. From top to bottom these measurements correspond to a uniaxial stress(strain) of 120kPa(35%), 7.4kPa(23%), 1kPa(15%) and 0kPa(3.8%). Unless shown, the error falls within the marker symbol

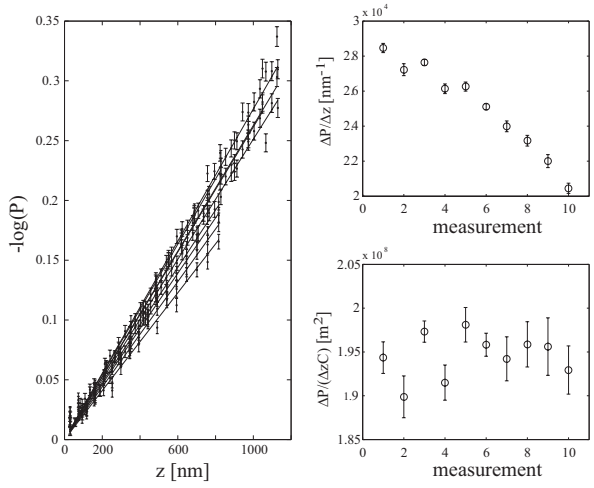

FIG. 5: The initial slopes of the polarisation. The slopes are proportional to the grain packing-fraction and the sample thickness multiplied by a constant. Dividing out the known thickness and the packing fraction ($C = \phi_{grain}(1-\phi_{grain})t$) should yield a constant term for all measurements. This analysis makes it possible to determine the grain density and consequently the grain packing fraction

$$\phi_{grain} = \frac{\rho_{sample}}{\rho_{grain}}. \tag{16}$$

Where ρ_{sample} is the density of the powder packing. The final amplitude of the polarisation (saturation level) is given by Eq. 9 and is read at a spin-echo length z related to ξ. Thus, the gradient of the initial part of $P(z)$ vs z yields a quantity only depending on the sample-thickness and sample composition, independent on structural arrangement.

$$-\frac{d\log(P)}{dz} \simeq t\lambda^2\Delta\rho_0^2\phi(1-\phi). \tag{17}$$

The grain density can now be estimated from the initial slopes of the experiments (see Fig. 5). Thus, dividing the values of the slopes with sample thickness and the primary particle packing-fraction ϕ_{grain} should yield a constant term for all experiments (see bottom right figure in Fig. 5). The constant term is composed of the neutron wavelength and the scattering length density according to Eq. 8.

This analysis gives a density of ρ_{grain}=1.1g/cm^3 and packing fractions ranging from ϕ_{grain}=0.34 up to ϕ_{grain}=0.53 for the highest strain.

C. Curve shapes and their amplitudes

For a more complete analysis of the SESANS experiment we apply a model that describes an autocorrelation function of the density distribution. From that model we are able to calculate the corresponding projection as well as the expected polarisation -shapes and amplitudes.

The thickness t, packing fraction ϕ, neutron wavelength λ are all known experimental parameters that contribute to the saturation level. The scattering length density $\Delta\rho_0$ is a constant parameter given by the chemical composition of the sample. Thus, in order for the model to be consistent it has to yield a constant scattering length-density term for all ten measurements. In short, we have to find a model capable of describing both the shape and the correlation length ξ of $\gamma(r)$, producing the saturation level observed in the measurement.

To model the data we use the von Karman correlation function, which describes a statistical self affine density distribution according to Eq:s 11, 12 and 13. The model explains the microstructure with two parameters, the Hurst number H and a characteristics size a of the density distribution. This yields, including experimental parameters, a scattering length density of about 1.1×10^{14}m^{-2} for all samples.

We extract two parameters from the model, the Hurst exponent H and the characteristic size a of the heterogeneities. The characteristic size is decreasing with increasing strain. In order for the powder to be compressed the larger inhomogeneities, clusters and voids have to be broken and collapsed. This first stage occurs at the lower stress amplitudes and produces relatively large changes in a. When the larger and weaker heterogeneities have collapsed and produced a denser structure any further densification is created by the rearrangement of primary grains. This latter stage is governed by higher stresses and smaller changes in the characteristic size of the het-

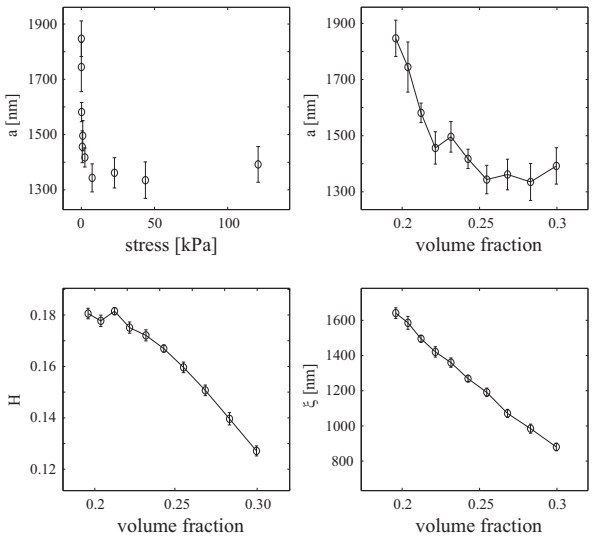

FIG. 6: Extracted fit parameters according to Eq. 7 together with stress-strain curve for the silica powder. The model shows that the characteristic size a as well as the hurst exponent decreases as a function of compression. Consistent with the formation of a more space filling structure. The volume fractions are here expressed in terms of the skeleton-packing fraction ϕ_{sk}

erogeneities. This "hard-core" behaviour is illustrated when we plot the characteristic size a versus the stress in Fig. 6, where we see how a reaches a sudden limit around 1300nm and no further changes is seen for higher stresses. All together we see that the decrease in microscopic length scale a corresponds well with the total final strain, both being around 30%

The Hurst exponent is decreasing with increasing strain, consistent with the formation of a space filling structure. The Hurst exponent contributes to the shape of the curve as well as to the final level of the polarisation.

V. CONCLUSIONS

A stress strain measurement was conducted simultaneously with a microstructural investigation on a cohesive silica powder (Sipernat-310). The microstructure was characterised in terms of the autocorrelation function of the density distribution.

The primary grain density could be determined by analysing the initial slopes of the measurements. This yielded a factor of two lower density as compared to the skeleton density of pure silica. The grain density was used to calculate the packing fraction of grains contained in the sample. We observe a divergence in the stress versus packing-fraction at around 0.50.

We are able to follow the fractal nature of the powder in terms of the so called Hurst exponent. We see that a more space filling structures, low Hurst numbers, are formed when increasing the strain.

When straining the sample the larger heterogeneities such as clusters and voids will break up and collapse, this process requires a lower stress amplitude. Further densification is governed by the movement and rearrangement of primary grains which is harder to achieve and calls for higher stresses. This can be seen in the non-linear decay of the typical size a with strain and is also found in the exponential behaviour of the stress-strain response curve. Comparing the beginning and the end of the experiment we see that the decrease in microscopic length scale a corresponds well total applied strain, both being around 30% for the whole experiment.

VI. ACKNOWLEDGMENTS

We thank Chris Duif at the Reactor Institute Delft for valuable discussions and help with performing the experimental part of this work. This work is part of the research programme of the 'Stichting voor Fundamenteel Onderzoek der Materie (FOM)', which is financially supported by the 'Nederlandse Organisatie voor Wetenschappelijk Onderzoek (NWO)'.

[1] J. Tomas, Granular Matter **6**, 75 (2004).
[2] T. Aste, M. Saadatfar, and T. Senden, Physical Review E **71** (2005).
[3] P. Richard, P. Philippe, F. Barbe, S. Bourlès, X. Thibault, and D. Bideau, Physical Review E **68** (2003).
[4] G. Seidler, G. Martinez, L. Seeley, K. Kim, E. Behne, S. Zaranek, B. Chapman, S. Heald, and D. Brewe, Physical Review E **62**, 8175 (2000).
[5] A. Sederman, P. Alexander, and L. Gladden, Powder Technology **117**, 255 (2001).
[6] D. Mueth, G. Debregeas, G. Karczmar, P. Eng, S. Nagel, and H. Jaeger, Nature **406**, 385 (2000).
[7] W. G. Bouwman, O. Uca, S. V. Grigoriev, W. H. Kraan, J. Plomp, and M. T. Rekveldt, J. Appl. Phys. A **74**, S115 (2002).
[8] R. A. Andersson, W. G. Bouwman, and I. M. de Schepper, in *Powders and Grains* (Stuttgart, Germany, 2005),

pp. 13–15.
[9] T. Krouglov, I. M. de Schepper, W. G. Bouwman, and M. T. Rekveldt, Journal of Applied Crystallography **36**, 117 (2003).
[10] H. Tromp, C. de Kruif, and W. G. Bouwman, Food colloids **826**, 87 (2006).
[11] L. Klimes, Pure and Applied Geophysics **159**, 1811 (2002).
[12] B. B. Mandelbrot, *The Fractal Geometry of Nature* (W.H. Freeman and Company, San Fransisco, 1982).
[13] L. Feigin and D. Svergun, *Structure Analysis by Small-Angle X-Ray and Neutron Scattering* (Plenum Press, 1987).
[14] R. Gähler, R. Golub, K. Habicht, T. Keller, and J. Felber, Physica B **229**, 1 (1996).
[15] M. T. Rekveldt, J. Plomp, W. G. Bouwman, and W. H. Kraan, Rev. Sci. Instr. **76** (2005).
[16] P. Debye and A. M. Bueche, Journal of Applied Physics **20**, 518 (1949).
[17] P. Debye, H. R. Andersson, and H. Brumberger, Journal of Applied Physics **28**, 679 (1957).
[18] P. Wong and Q. Cao, Physical Review B **45**, 7627 (1992).
[19] M. Hunter, V. Backman, G. Popescu, M. Kalashnikov, C. W. Boone, A. Wax, V. Gopal, K. Badizadegan, G. D. Stoner, and M. Feld, Physical Review Letters **97**, 1 (2006).